이학석사학위논문

Lower Critical Solution Temperature (LCST) Phase Separation of Glycol Ethers for Forward Osmotic Control

2014 년 2 월

서울대학교 대학원

화학부 생화학 전공

Daichi Nakayama

Lower Critical Solution Temperature (LCST) Phase Separation of Glycol Ethers for Forward Osmotic Control

지도교수 이 연

이 논문을 이학석사학위논문으로 제출함

2014 년 2 월

서울대학교 대학원

화학부 생화학 전공

Daichi Nakayama

Daichi Nakayama 의 석사학위논문을 인준함

2014 년 2 월

위 원 장 _____ (인)

부 위 원 장 _____ (인)

위 원 _____ (인)

Abstract

Lower Critical Solution Temperature (LCST) Phase Separation of Glycol Ethers for Forward Osmotic Control

Daichi Nakayama
Department of Chemistry
College of Natural Science
The Graduate School
Seoul National University

Lower critical solution temperature (LCST) phase transition of glycol ether (GE)/water mixtures induces abrupt change of osmotic pressure driven by mild temperature change. The temperature-controlled osmotic change was applied for the forward osmotic (FO) desalination. Among evaluated three GEs, di(ethylene glycol) *n*-hexyl ether (DEH) was selected as a potential FO draw solute. A DEH/water mixture with a high osmotic pressure could draw fresh water from a high-salt feed solution such as seawater through a semipermeable membrane at around 10 °C. The water-drawn DEH/water mixture was phase-separated into a water-rich phase and a DEH-rich phase

at around 30 °C. The water-rich phase with a much reduced osmotic pressure released water into a low-salt solution, and the DEH-rich phase was recovered into the initial DEH/water mixture. The phase separation behaviour, the residual GEs concentration at the water-rich phase, the osmotic pressure of the DEH/water mixture, and the osmotic flux between DEH/water mixture and salt solutions were carefully analysed for FO desalination. The liquid-liquid phase separation of the GE/water mixture driven by the mild temperature change between 10 °C and 30 °C is very attractive for the development of an ideal draw solute for future practical FO desalination.

Keyword: thermo-sensitive materials, lower critical solution temperature (LCST), glycol ether, phase diagram, desalination.

Student number: 2011-24025

Contents

1. Introduction

Earth is facing an impending water shortage due to increasing water pollution and progressing desertification [1]. Seawater, which accounts for 97% of all the water on Earth, is an attractive source of potential fresh water, and more than 40,000,000 m^3 of seawater are desalinated worldwide every day [2]. Distillation and reverse osmosis (RO) are the two primary methods for obtaining fresh water, but forward osmosis (FO) is an emerging technique for energy-efficient desalination [3]. The FO method uses a draw solution with a higher concentration than the feed solutions, *i.e.*, seawater, which can spontaneously 'draw' fresh water from the feed solution through a semipermeable membrane. Fresh water can be recovered from the diluted draw solution following the removal of the draw solute by various methods.

A FO system employing ammonium bicarbonate/ammonium hydroxide (NH_4HCO_3/NH_4OH) as draw solutes has been extensively studied for practical desalination applications (Fig. 1, left) [4]. After withdrawing water from the feed solutions, the draw solutes decompose into ammonia (NH_3) and carbon dioxide (CO_2), which exhibit liquid-gas (L-G) phase separation from water upon heating to approximately 60 °C. The NH_4HCO_3/NH_4OH-based FO system is now in the pilot stage, but several problems must be overcome to achieve distillation and RO in practical desalination applications [5]. For example, the decomposition step requires considerably elevated temperatures, the separation and recovery of the gaseous draw

solutes require complex equipment for distillation and re-condensation, and the strongly basic pH of the draw solution can potentially damage the semipermeable membrane although thin film composite (TFC) membranes comprising a polyamide selective layer have recently been developed and partially overcome the vulnerability at the basic conditions [6]. Various materials, including inorganic salts [7], magnetic nanoparticles [8], and hydrogels [9], have been explored as substitutes for NH_4HCO_3/NH_4OH, but these materials require complex discontinuous desalination processes or exhibit very limited osmotic drawing powers that allow only limited water withdrawal, even from low-salt saline solutions (<0.035 m NaCl).

There are several requirements for an ideal draw solute. First, the solute should exhibit high aqueous solubility to achieve high drawing powers because the osmotic pressure (π) is related to the molality of the solution (m), as described by a virial expansion of the Morse equation (1):

$$\pi = \rho RT\,(m + Bm^2 + Cm^3 + \ldots) \qquad (1)$$

where is density, R is the gas constant, T is temperature, B is the osmotic second virial coefficient and C is the osmotic third virial coefficient. Second, the solute should possess a low molar mass because the molar mass is inversely related to the molality or osmotic pressure except for polyelectrolyte molecules with a large amount of counter-ions. Third, the draw solutes should be separated by mild temperature changes, preferably induced by waste heat or sunlight. Fourth, the separation and recovery

should be simple and efficient, and residual draw solute should be minimised in the separated water. Fifth, it will be more acceptable if the draw solution exhibits neutral pH values to reduce potential damages to the membrane.

In my study, I aimed to develop a FO system employing draw solutes with the desirable characteristics mentioned above (Fig. 1, right). Lower critical solution temperature (LCST) materials [10] were selected as candidates for the draw solutes. At temperatures below the phase transition temperature, LCST materials are miscible with water at high concentrations, enabling the efficient withdrawal of water from feed solutions. The water-drawn solution is subsequently transferred to an environment at a higher temperature than the phase transition temperature. At this elevated temperature, the LCST material exhibits liquid-liquid (L-L) phase separation from water, reducing the effective concentration of the draw solution. The phase-separated draw solution with a decreased effective concentration can then spontaneously release water into a low-salt solution. Because the phase transition temperature of LCST materials can be controlled by altering the chemical structure [11], the energy requirement for the separation of draw solutes can be greatly reduced by using a LCST material with a low phase transition temperature. Moreover, the L-L phase-separated LCST material can be recovered into the original draw solution through a simple liquid-liquid separator without the need for a complex re-condensation process of gaseous draw solutes. It was recently reported that a desalination method

through L-L phase separation of switchable polarity solvents, but gaseous CO_2 was also required as a stimuli for the polarity change [12].

In previous report, it was demonstrated that the osmotic pressure can be effectively controlled by the LCST phase transition of a low-molar-mass *N*-acylated amine derivative [13]. In this study, I suggest glycol ethers (GEs) as suitable draw solutes for FO. Many low-molar-mass GEs are miscible with water at all concentrations below the phase transition temperature [14], allowing the generation of sufficient osmotic pressure to draw water from seawater. These GEs can be phase-separated at approximately 30 °C, which is significantly lower than the decomposition temperature of ammonium bicarbonate [4]. Aqueous solutions of GEs with hydroxyl- and ether-based structures exhibit neutral pH values, reducing the potential damage to the membrane. In addition, the low viscosities of GEs [15] can be beneficial in establishing circulation processes [16], and their facile synthesis makes them amenable to commercialisation.

By evaluating the temperature-sensitive L-L phase separation of different GE/water mixtures, I examined the use of GEs as draw solutes in detail. In particular, the effective concentration or osmolality was analysed in the GE/water mixture to compare the power of osmotic withdrawal, water flux, and the final salt concentration of the resulting water.

2. Experimentals and Methods

2-1. LCST draw solutes

Di(ethylene glycol) *n*-hexyl ether (DEH) and propylene glycol *n*-butyl ether (PB) were purchased from Sigma-Aldrich, USA. Di(propylene glycol) *n*-propyl ether (DPP) was kindly donated from Dow Chemical, USA.

2-2. Measurements of LCST phase transition

The LCST phase transitions of the GE aqueous solutions were measured using a Jasco (Japan) Model V-650 UV-VIS spectrophotometer at a wavelength of 600 nm. The phase transition temperature was determined based on the transmittance change with elevating temperature. The phase transition temperature was defined as the temperature at which the transmittance was below 95%.

2-3. Concentrations of the GE-rich phase and water-rich phase following phase separation

The concentrations of the GE-rich phase and water-rich phase following phase separation at 30 °C, 40 °C, and 50 °C were measured by ^{1}H-NMR. After a 1 hour relaxation of 30 w/w % (weight of GE / weight of GE and water) GE solutions at each temperature in an oil bath, the GE-rich phase and water-rich phase were carefully collected in a glass tube. The

concentration of the GE in each phase was determined by ^{1}H-NMR using a set quantity of acetic acid as an internal standard.

2-4. Measurement of osmolality

The osmolality of the DEH/water mixture at various concentrations was measured using freezing point depression osmometry (Semi-Micro Osmometer K-7400, Knauer Inc., Germany) and vapour pressure depression osmometry (Vapor Pressure Osmometer K-7000, Knauer Inc., Germany). In case of the vapour pressure osmometry, the osmolalities of the samples were measured at 30 °C, 40 °C, and 50 °C.

2-5. Temperature-controlled water withdrawal and release

FO flux experiments were performed using cross-flow circulating module referring to Cath *et al* [17]. The glass cell consists of two channels; one on each side of the cellulose triacetate membrane (Hydration Technology Innovation, USA). Feed and draw solution flowed concurrently through respective cell at the same flow rate of 700 mL/min. The selective layer of the semipermeable membrane faced the GE solution. The osmotic water flux from the NaCl solution to the GE solution was calculated from the weight change of each solution over a 1 h period following 1 h of stabilisation at 10 (±2) °C. The reversed osmotic flux from the phase-separated GE solution to the NaCl solution was similarly calculated at 30 (±2) °C.

3. Results and Discussion

3-1. Phase separation behaviour of glycol ethers (GEs)

To achieve high osmotic pressures, I selected GEs with molar masses below 200 g/mol, including di(ethylene glycol) *n*-hexyl ether (DEH), di(propylene glycol) *n*-propyl ether (DPP), and propylene glycol *n*-butyl ether (PB) (Fig. 2). The physical characteristics of DEH, DPP, and PB are summarised in Table 1.

At a given composition and pressure, LCST phase separation occurs when the Gibbs free energy of mixing ($\Delta G_m = \Delta H_m - T\Delta S_m$) becomes zero as the negative entropy of mixing (ΔS_m) due to hydrophobic interactions and the ordering of water molecules around the solutes becomes dominant over the negative enthalpy of mixing (ΔH_m) upon reaching a specific temperature [18]. Also, the phase separation occurs at the composition (χ) where the second and third derivatives of ΔG_m with respect to the composition are both equal to zero ($\partial^2 \Delta G_m / \partial \chi^2 = 0$; $\partial^3 \Delta G_m / \partial \chi^3 = 0$) at a given temperature and pressure [19].

The GEs were expected to exhibit a LCST transition because the hydrophilic oligoglycol moieties and the hydrophobic alkyl groups were well-balanced in its molecular structure. Notably, modulation of the phase transition temperature is possible because various types of GEs can be synthesised using Williamson ether synthesis to display different oligoglycol and alkyl moieties [20].

Phase diagrams of the aqueous mixtures with DEH, DPP, and PB are shown in Figure 3. The DEH/water and DPP/water mixtures exhibited U-shaped phase diagrams with one-phase miscibility at low temperatures and two-phase separation at high temperatures (Fig. 3a and 3b). However, the PB/water mixture exhibited one-phase miscibility at both low and high concentrations of PB and two-phase separation in the middle at all temperatures between 0 °C and 100 °C (Fig. 3c). For DEH and DPP, the phase transition from one phase to two phases occurs at approximately 20 °C for a wide range of compositions. Highly concentrated GE solutions can be prepared at temperatures below the phase transition temperature to generate sufficient osmotic pressure to draw water from high-salt solutions such as seawater (0.62 m NaCl equivalent). When the temperature of the GE solutions increases beyond the phase transition temperature, they become phase-separated into two liquid phases, a GE-rich phase and a water-rich phase. Molality-based phase diagrams of the GE/water mixtures are also shown in Figure 4.

An FO process was suggested based on the phase separation diagram of the GEs (Fig. 5). A GE mixture with a higher osmotic pressure than the feed solutions draws water through a semipermeable membrane at low temperatures (low T) (a). The diluted GE mixture is then transferred to a high-temperature (high T) environment (b). The GE mixture is phase-separated into an upper GE-rich phase and a lower water-rich phase at high T (c). The lower water-rich phase with significantly reduced osmotic

pressure releases water into a lower-salt solution through the second semipermeable membrane (d). The upper GE-rich phase is transferred to the low T environment to close the FO cycle (e). Along with the cycle from (a) to (e), water withdrawal, water release, and GE recovery proceed simultaneously. Because the phase transition temperatures of DEH and DPP are approximately 20 °C, it was expected that the FO cycle could be operated near room temperature or between 10 °C and 30 °C, far lower than the operation temperatures of other FO systems [4, 9].

3-2. Composition of GEs in water- and GE-rich phases

The osmotic pressure of GE/water mixtures at low T determines the maximum drawable salt concentration of the feed solution (Fig. 5(a)). After the phase separation at high T, the osmotic pressure of the lower water-rich phase determines the minimal salt concentration of the product water where the water-rich phase can release water into (Fig. 5(d)). On the other hand, the upper GE-rich phase can maintain the osmotic pressure of the drawing solution at low T through the recovery process (Fig. 5(e)). The osmotic pressure can be predicted with partial accuracy by the measurement of the composition of each phase. The composition of a one-phase GE/water mixture at low T is determined by the amount of dissolved GE. On the other hand, the composition of the water-rich phase and the GE-rich phase at high T can be predicted from the phase diagram, in which the points on the phase separation line indicate the compositions of the separated phases. The

composition of each phase at 30, 40, and 50 °C was measured using ^{1}H-NMR and compared with the value predicted from the phase diagram (Table 2). The two methods produced similar results, particularly for the concentrations of the water-rich phase.

Among the GEs, DEH showed preferable concentration difference between water- and GE-rich phases. The DEH concentration in the GE-rich phase was similar with other GEs, but the concentration in the water-rich phase was several-fold lower. Because of the lower concentration in the water-rich phase for the product water with lower salt concentration, I selected DEH as a potential draw solute for further study in next FO experiments.

3-3. Osmotic pressure in DEH/water mixtures

Although the concentration of the GEs could be known both in the homogeneous mixtures at low T and the water-rich phase at high T, the corresponding osmotic pressure is not directly proportional to the concentrations of the GEs. Therefore, the osmotic pressure of the DEH/water mixtures at various compositions was measured using two types of osmometers based on the depression of the freezing point and vapour pressure. The former was used for estimating osmotic pressures of homogeneous mixtures at low T near the freezing point, and the latter was used for estimating osmotic pressures of water-rich phase at high T with varying temperatures.

The osmotic pressure of homogeneous DEH/water solution at low T is

shown in terms of osmolality in Figure 6a. At low concentrations below 0.11 m, the osmolality was almost proportional to molality, which is a typical behaviour of dilute solutions. However, the slope decreased drastically at intermediate concentrations. It represents the osmotic second virial coefficient (*B* in Eq. (1)) of the DEH/water mixtures is negative, and the DEH-DEH solute interaction is significantly high [21]. Then, the slope increased again, and 7.8 m DEH solution showed 3.0 Osm/Kg, which is around 3 times higher than that of seawater. The osmotic third virial coefficient (*C* in Eq. (1)) is positive, showing that higher order interactions between solute molecules are significant at high concentrations.

The osmotic pressure of water-rich phase at high T is shown in Figure 6b. The osmolality was almost proportional to molality at low concentrations, but it was saturated near the phase separation points. The decrease of the slope represents the solute-solute interaction increased as the concentration increased. LCST mixtures exhibit a certain constant vapour pressure with varying compositions in the phase-separated region because the compositions of the solvent-rich phase and the solute-rich phase are constant although their relative amounts are different. Therefore, I could reliably assume that the saturated value of the osmolality was close in value to the actual osmolality of the water-rich phase following phase separation at each temperature. The osmolality-molality relationship of DEH/water mixtures is quite similar to that of triethylamine (TEA)/water mixtures, a classical example of the LCST mixture [22].

The saturated osmolality was inversely related to temperature. The saturated osmolalities of the DEH/water mixtures were 0.060, 0.050, and 0.045 Osm/kg at 30, 40, and 50 °C, respectively. Because the concentrations of the water-rich phases of the phase-separated DEH/water mixtures at high T were also inversely related to temperature (Table 2), the decrease in the saturated osmolality was expected. Because the osmotic pressure of the water-rich phase determines the minimum salt concentration of the resulting water, as mentioned above, the lower osmolality of the water-rich phase in the DEH/water mixtures is remarkably beneficial in reducing the final salt concentration. For example, the osmolality of the water-rich phase in the DEH/water mixtures at 30 °C (0.060 Osm/kg) was similar to that of a 0.025 m NaCl solution; six times lower than physiological saline (0.15 m). Theoretically, an approximately 0.025 m NaCl solution can be produced from seawater (0.62 m NaCl equivalent) through a DEH-based FO system without any additional reverse osmotic pressure.

3-4. Osmotic water withdrawal and release

The osmotic water withdrawal from high-salt NaCl solutions at low T and the subsequent water release into low-salt NaCl solutions at high T were examined to demonstrate the feasibility of GEs as draw solutes in FO. Based on the phase diagrams of DEH, I selected low and high temperatures of 10 and 30 °C, respectively.

Figure 7a displays the osmotic water flux from NaCl solutions to the DEH

draw solutions through a semipermeable membrane at 10 °C expressed as litres per square meter per hour (L m^{-2} h^{-1}; LMH). Due to the miscibility of DEH with water at 10 °C, the concentration of DEH could be freely selected. To make the process amenable to repeated cycling, I selected a DEH draw solution of 12 m (70 w/w %) because this value is the concentration of DEH in the solute-rich phase at 30 °C (Table 2). The water flux toward the draw solution increased as the concentration gradient increased. The DEH draw solution was able to draw water from a seawater equivalent solution (0.62 m NaCl) with a flux of 0.62 LMH.

Figure 7b depicts the osmotic water release from the water-rich phase into NaCl solutions at 30 °C. The concentrations of the water-rich phases in the DEH mixtures at 30 °C (0.081 m) were used as the operating concentrations for water release. The DEH water-rich phase was able to release water to a 0.15 m NaCl solution (equivalent to physiological saline). It was also able to release fresh water to even 0.050 m NaCl solutions. Comparing the osmolality of DEH with that of NaCl at 30 °C (Fig. 6b and Fig. 8), the water release from the water-rich phase into the low-salt NaCl solution was quite satisfactory.

3-5. Water production yield based on the phase diagram and selection of ideal temperature-sensitive draw solutions

Desalinated water production through the temperature-sensitive osmotic system can be estimated based on the phase diagram of the draw solution

(Fig. 9). For the recycling, I would start from the draw solution with the concentration of C_s, the concentration of the solute-rich phase at T_{high}. The drawing solution is diluted through the drawing process. At the maximum dilution, the concentration would finally reach to C_{eq}, the concentration with an equal osmotic pressure with the feed solution. Then, the diluted draw solution is heated to T_{high}, and the solution was phase-separated into two phases, a solute-rich phase with a concentration of C_s and a water-rich phase with a concentration of C_w. The relative ratio between the solute-rich phase and the water-rich phase is amount of two phases is α:β, from the lever rule [23]. Water molecules in the water-rich phase are osmotically transferred to mild saline. As water is released, the amount of water-rich phase is decreased gradually. In this step, C_w and C_s are maintained and only the relative ratio between two phases changes to α':β'. The amount of the solute-rich phase increases, while the amount of the water-rich phase decreases. Finally, the solute-rich phase can be re-used as a draw solution for the second cycle after cooling to T_{low}.

For the drawing from the feed solution, C_{eq} should be lower than C_s. Also, the dilution below C_w is meaningless because the drawing solution cannot be phase-separated at T_{high} ($C_w < C_{eq} < C_s$). For the water release, the osmotic pressure of C_w should be lower than the osmotic pressure of the mild saline. Therefore, the minimum concentration of the product water is determined by the C_w.

Through the whole cycle, I could obtain a low-salt solution equivalent to a

C_w-draw solution from a high-salt solution equivalent to a C_{eq}-draw solution. If the difference between C_{eq} and C_w is large, I can obtain a much diluted product water, but at the same time, the amount of product water becomes small due to the high α:β ratio. Reversely, if difference between C_{eq} and C_w is small, I can obtain a large amount of product water due to the low α:β ratio, but the dilution factor should be small. Therefore, I should choose an appropriate draw solute according to the objective.

Four important characteristics for an ideal temperature-sensitive draw solution can be partially predicted from the phase diagram: the maximum solubility or osmolality at low T, the phase separation temperature, the concentration (C_w) or osmolality of the water-rich phase at high T, and the concentration of the solute-rich phase at high T (C_s).

Because the maximum solubility or osmolality at low T determines the maximum drawable concentration of the feed solution, miscibility over a wide range of concentrations of DEH/water mixtures is highly valuable. In this study, a seawater equivalent saline was drawable using the DEH-based draw solutions.

The phase separation temperature determines the operating temperature gradient. Because the energy efficiency of an FO system is largely dependent on the operating temperature for separation (high T), the ability to conduct phase separation near room temperature is very attractive. In this study, 10 and 30 °C were chosen as the low T and high T, temperatures which are readily achievable using sunlight-induced diurnal temperature

changes or waste heat from factories or power plants.

As described above, C_w and C_s determines the minimum concentration and the amount of product water (or the α:β ratio). The solute-rich phase is recovered into the draw solution by circulation, and the water-rich phase releases water into the product water through a semipermeable membrane. The lower the C_w, the lower the concentration of the final product water *via* spontaneous osmosis. The higher the C_s, the larger the amount of the product water due to the low α:β ratio.

In this study, an approximately 0.050 m NaCl solution was readily obtained from the water-rich phase by spontaneous osmosis from a seawater equivalent. It is expected that fresh water-grade salt solutions (<0.010 m) can be obtained using this method given the future discovery of temperature-sensitive materials with lower residual concentrations in the water-rich phase (*i.e.*, exhibiting C_w that are much closer to the *y*-axis). Of course, final product water with a much lower salt concentration can be obtained by other methods, including reverse osmosis (RO). Because the osmotic pressure of the water-rich phase of the DEH/water mixtures at 30 °C is approximately 1.6 atm, the RO process can produce fresh water at much lower operating pressures compared with the pressures required in direct RO from seawater (> 27 atm). In addition, larger amount of water can be obtained per each cycle using temperature sensitive materials with a low α:β ratio from higher C_s.

4. Conclusions

To overcome the limitations of current FO desalination systems based on liquid-gas phase separation, I developed a FO control based on the LCST liquid-liquid phase separation of GEs by mild temperature changes. Water was drawn from a seawater equivalent at 10 °C and released into a low-salt saline (approximately 0.05 m) at 30 °C using the GE-based draw solutions. The phase diagram-based approach will be helpful in the future development of ideal draw solutes with high solubilities at low T, mild phase transition temperatures, low C_w and high C_s. Practical FO desalination can be achieved in the near future with the development of various draw solutes and advanced membranes exhibiting higher water flux and higher rejection [24].

References

[1] J. F. Reynolds, D. M. Stafford Smith, E. F. Lambin, B. L. Turner, M. Mortimore, S. P. J. Batterbury, T. E. Downing, H. Dowlatabadi, R. J. Fernandez, J. E. Herrick, E. Huber-Sannwald, H. Jiang, R. Leemans, T. Lynam, F. T. Maestre, M. Ayarza and B. Walker, *Science*, 2007, **316**, 847; C. J. Vörösmarty, P. B. McIntyre, M. O. Gessner, D. Dudgeon, A. Prusevich, P. Green, S. Glidden, S. E. Bunn, C. A. Sullivan, C. Reidy Liermann and P. M. Davies, *Nature*, 2010, **467**, 555.

[2] R. F. Service, *Science*, 2006, **313**, 1088; Q. Schiermeier, *Nature*, 2008, **452**, 260; M. Elimelech and W. A. Phillip, *Science*, 2011, **333**, 712.

[3] R. E. Karavath and J. A. Davis, *Desalination*, 1975, **16**, 151; T. Y. Cath, A. E. Childress and M. Elimelech, *J. Membr. Sci*, 2006, **281**, 70; D. Li and H. Wang, *J. Mater. Chem. A*, 2013, **1**, 14049; Q. Ge, M. Ling, T.-S. Chung, *J. Memb. Sci.*, 2013, **442**, 225.

[4] J. R. McCutcheon, R. L. McGinnis and M. Elimelech, *Desalination*, 2005, **174**, 1; J. R. McCutcheon, R. L. McGinnis and M. Elimelech, *J. Membr. Sci.*, 2006, **278**, 114.

[5] R. L. McGinnis, N. T. Hancock, M. S. Nowosielski-Slepowron, G. D. McGurgan, *Desalination*, 2013, **312**, 67; N. T. Hancock, Engineered Osmosis for Energy Efficient Separations: Optimizing Waste Heat Utilization FINAL SCIENTIFIC REPORT DOE F 241.3 DE-EE0003467, 2013; J. E. Miller, L. R. Evans, *Sandia Report*, SAND2006-4634, Sandia

National Laboratories, California, 2006; R. Wang, L. Shi, C.Y.Y. Tang, S.R. Chou, C. Qiu and A.G. Fane, *J. Membr. Sci.*, 2010, **355**, 158; N. Ma, J. Wei, R. Liao and C. Y. Tang, *J. Membr. Sci.*, 2012, **405-406**, 149.

[6] N. Y. Yip, A. Tiraferri, W. A. Phillip , J. D. Schiffman and M. Elimelech, *Environ. Sci. Technol.*, 2010, **44**, 3812.

[7] Z. Liu, H. Bai, J. Lee and D. D. Sun, *Energy Environ. Sci.*, 2011, **4**, 2582.

[8] M. M. Ling, K. Y. Wang, and T.-S. Chung, *Ind. Eng. Chem. Res.*, 2010, **49**, 5869.

[9] D. Li, X. Zhang, J. Yao, Y. Zeng, G. P. Simonb and H. Wang, *Soft Matter*, 2011, **7**, 10048; D. Li, X. Zhang, J. Yao, G. P. Simonb and H. Wang, *Chem. Commun.*, 2011, **47**, 1710.

[10] R. B. Griffiths and J. C. Wheeler, *Phys. Rev. A*, 1970, **2**, 1047.

[11] H. Kim, S. Lee, M. Noh, S. H. Lee, Y. Mok, G. Jin, J.-H. Seo and Y. Lee, *Polymer*, 2011, **52**, 1367.

[12] P. G. Jessop, S. M. Mercera and D. J. Heldebrant, *Energy Environ. Sci.*, 2012, **5**, 7240; M. L. Stone, C. Rae, F. F. Stewart and A. D. Wilson, *Desalination*, 2013, **312**, 124.

[13] M. Noh, Y. Mok, S. Lee, H. Kim, S. H. Lee, G. Jin, J.-H. Seo, H. Koo, T. H. Park and Y. Lee, *Chem. Commun.*, 2012,**48**, 3845.

[14] S. P. Christensen, F. A. Donate, T. C. Frank, R. J. LaTulip and L. C. Wilson, *J. Chem. Eng. Data*, 2005, **50**, 869.

[15] X.-X. Li, W.-D. Zhou, X.-Y. Li, J.-L. Sun and Wei Jiang, *J. Mol. Liq.* 2009, **148**, 73.

[16] Y. Mok, D. Nakayama, M. Noh, S. Jang, T. Kim and Y. Lee, *Phys. Chem. Chem. Phys.*, 2013, **15**, 19510.

[17] T. Y. Cath, M. Elimelech, J. R. McCutcheon, R. L. McGinnis, A. Achilli, D. Anastasio, A. R. Brady, A. E. Childress, I. V. Farr, N. T. Hancock, J. Lampi, L. D. Nghiem, M. Xie, N. Y. Yip, *Desalination*, 2013, **312**, 31

[18] H. G. Schild, *Prog. Polym. Sci.*, 1992, **17**, 163.

[19] H. Bijl, in Liquid-liquid equilibria in binary (2-methoxyethanol + alkane) systems at pressures up to 4000 bar, Delft University Press, Delft, Zuidholland, Netherlands, 1984, pp. 10-12.

[20] A. Williamson, *Philosophical Magazine*, 1850, **37**, 350; S. Paul and M. Gupta, *Tetrahedron Lett.*, 2004, **45**, 8825.

[21] *J. Phys. Chem*. B 2001, **105**, 5262.

[22] L. D. Roberts and J. E. Mayer, *J. Chem. Phys.*, 1941, **9**, 852.

[23] D. A. McQuarrie and J. D. Simon, in Physical Chemistry: a molecular approach, University Science Books, Sausalito, 1997, ch.24, pp. 970-977.

[24] M. Kumar, M. Grzelakowski, J. Zilles, M. Clark and W. Meier, *Proc. Natl. Acad. Sci. U.S.A.*, 2007, **104**, 20719; H. G. Park, F. Fornasiero, J. K. Holt, C. P. Grigoropoulos and O. Bakajin, *Nano Today*, 2007, **2**, 22.; M.T. M. Pendergast and E. M.V. Hoek, *Energy Environ. Sci.*, 2011, **4**, 1946.; X. Song , Z. Liu and D. D. Sun, *Adv. Mater.*, 2011, **23**, 3256.; D. Cohen-Tanugi and J. C. Grossman, *Nano Lett.*, 2012, **12**, 3602.

Tables

Table 1 Physical characteristics of GE draw solutes.

Draw solutes	MW (g/mol)	Density[a] (g/ml)	m.p. (°C)	b.p. (°C)	Viscosity[b] (mPa·s)
DEH	190.28	0.935	-40	260	5.77
DPP	176.25	0.926	-75	213	3.25
PB	132.20	0.875	-80	170	2.37

[a]At 25 °C. [b]Viscosity was measured at 28.5 °C.

Table 2 The GE concentration in each phase after the phase separation.

Draw solutes		**GE concentrations after phase separation (w/w % / m)**					
		30 °C		40 °C		50 °C	
		PD[a]	NMR[b]	PD	NMR	PD	NMR
Water-rich phase	DEH	1.5 / 0.079	1.5 / 0.081	1.1 / 0.059	1.1 / 0.059	0.93 / 0.049	1.1 / 0.056
	DPP	16 / 1.1	13 / 0.82	9.9 / 0.63	8.3 / 0.51	7.3 / 0.45	7.5 / 0.46
	PB	5.0 / 0.40	4.7 / 0.37	3.9 / 0.30	3.7 / 0.29	3.6 / 0.28	3.4 / 0.27
GE-rich phase	DEH	53 / 5.8	70 / 12	62 / 8.4	75 / 16	67 / 11	79 / 19
	DPP	81 / 24	77 / 19	84 / 29	79 / 21	85 / 33	79 / 22
	PB	86 / 46	88 / 53	87 / 49	89 / 60	87 / 49	91 / 77

[a]Concentrations based on the phase diagram. [b]Concentrations measured by ^{1}H-NMR in GE/D_2O mixtures.

Figures

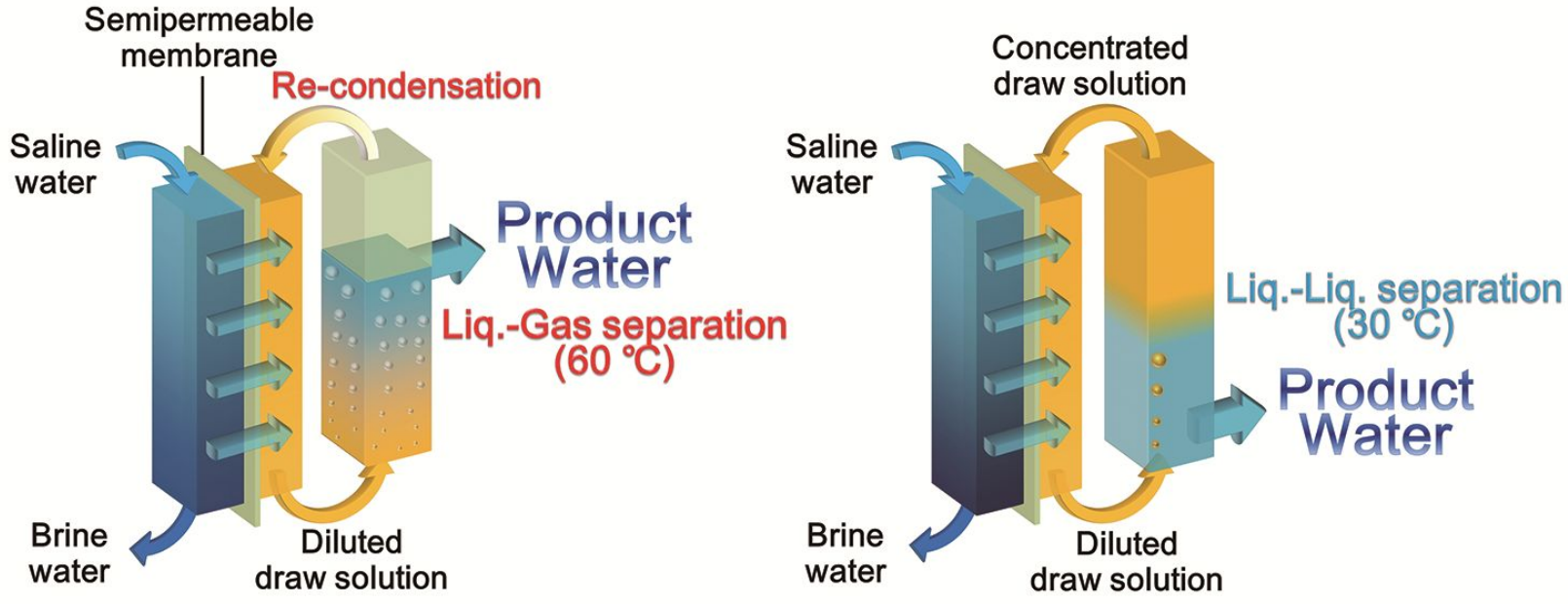

Fig. 1 Schematic illustration of the FO desalination systems based on a liquid-gas phase separation (left) and a liquid-liquid phase separation (right).

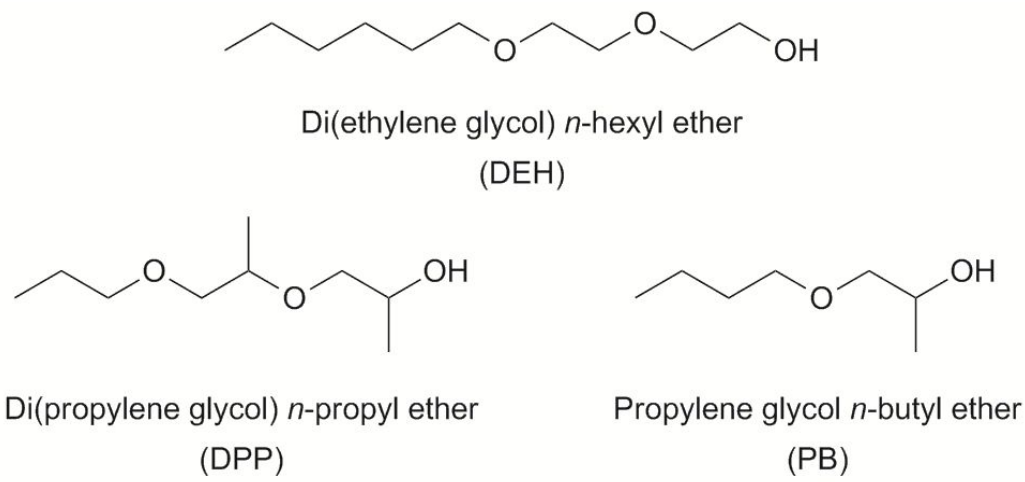

Fig. 2 Chemical structures of glycol ethers evaluated in this study.

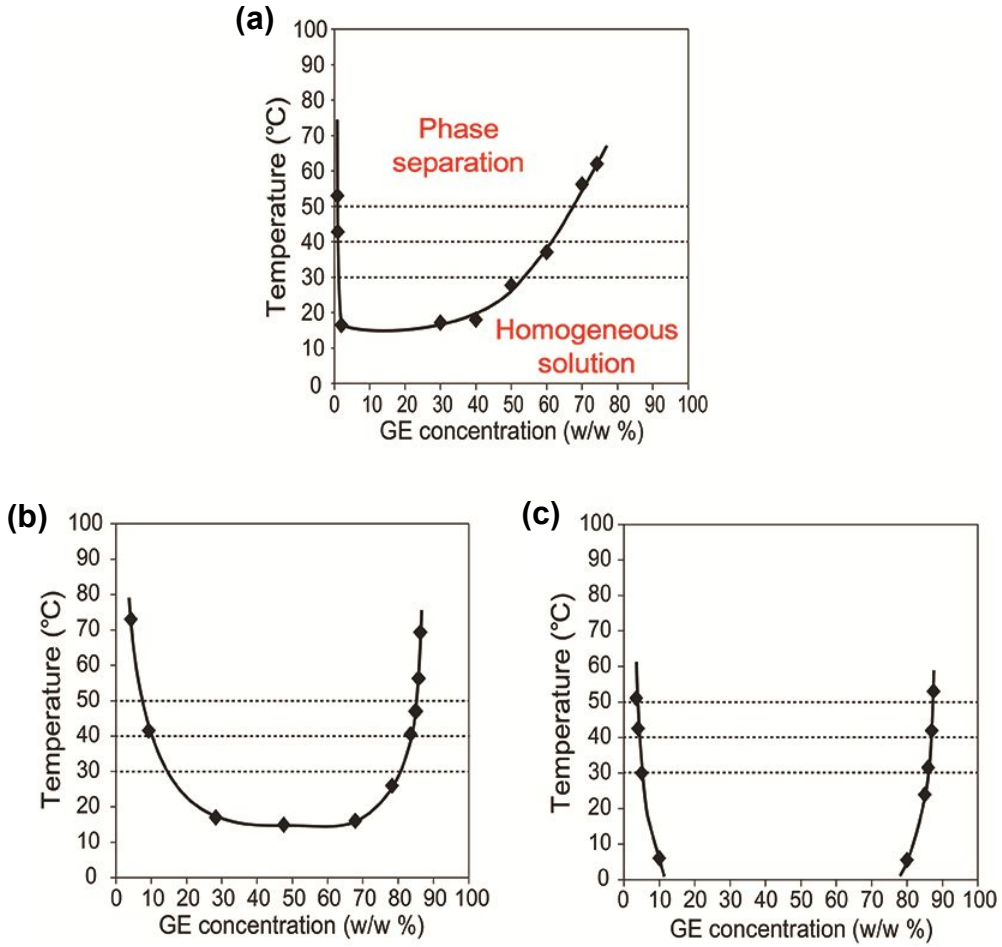

Fig. **3** Phase diagrams of GE-water mixtures; (a) DEH/water, (b) DPP/water, and (c) PB/water.

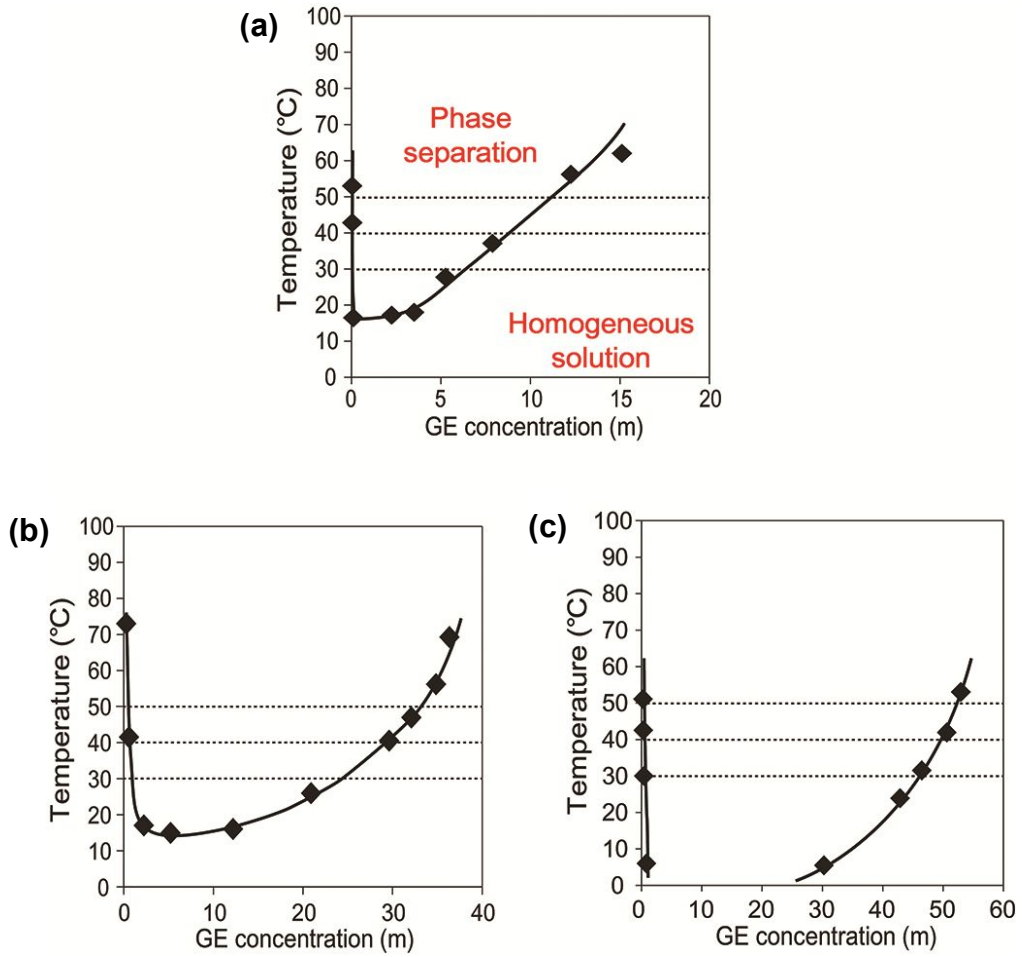

Fig. 4 Molality-based phase diagrams of GE-water mixtures; (a) DEH/water, (b) DPP/water, and (c) PB/water.

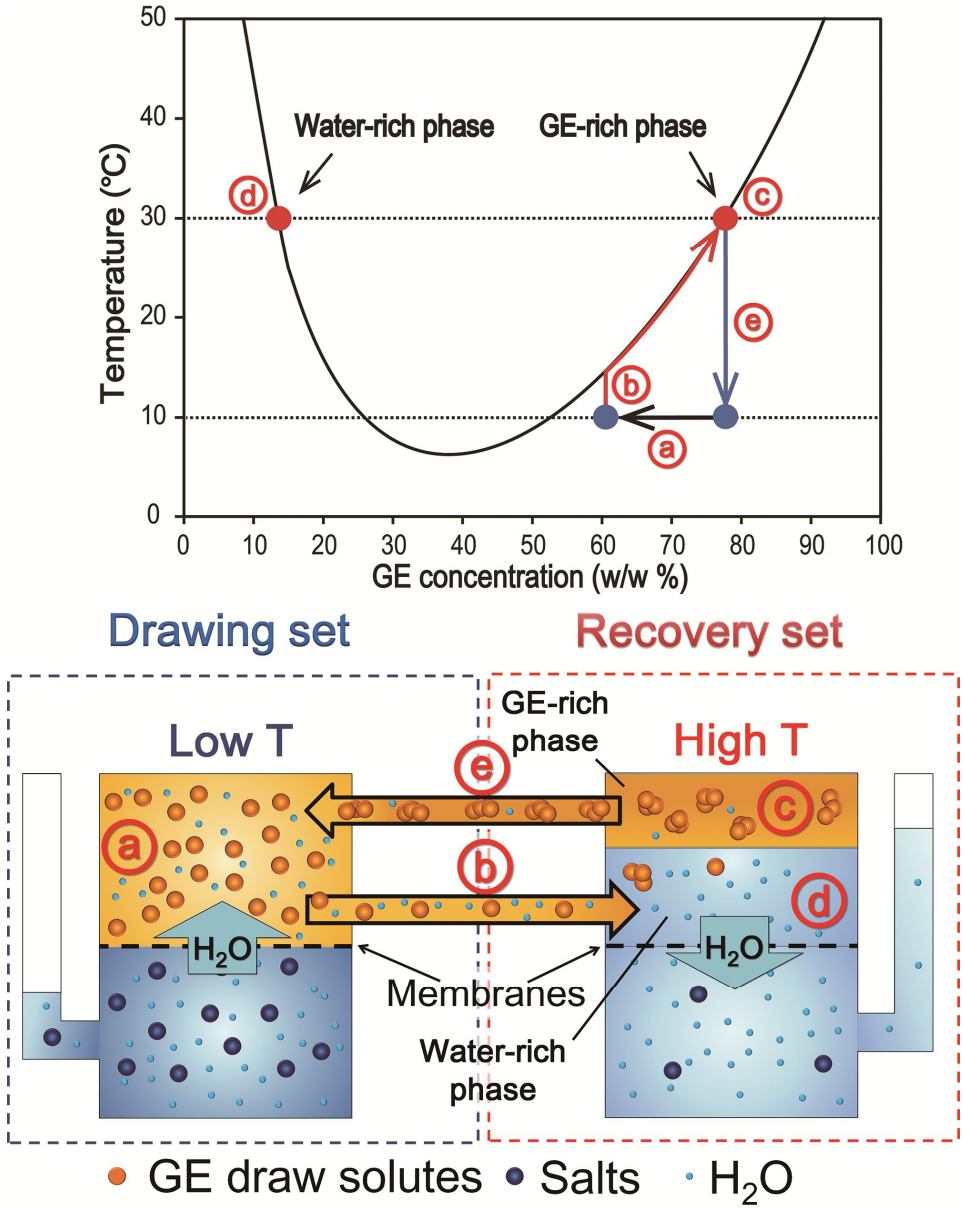

Fig. 5 A schematic diagram of a FO desalination system based on the GE/water phase diagram.

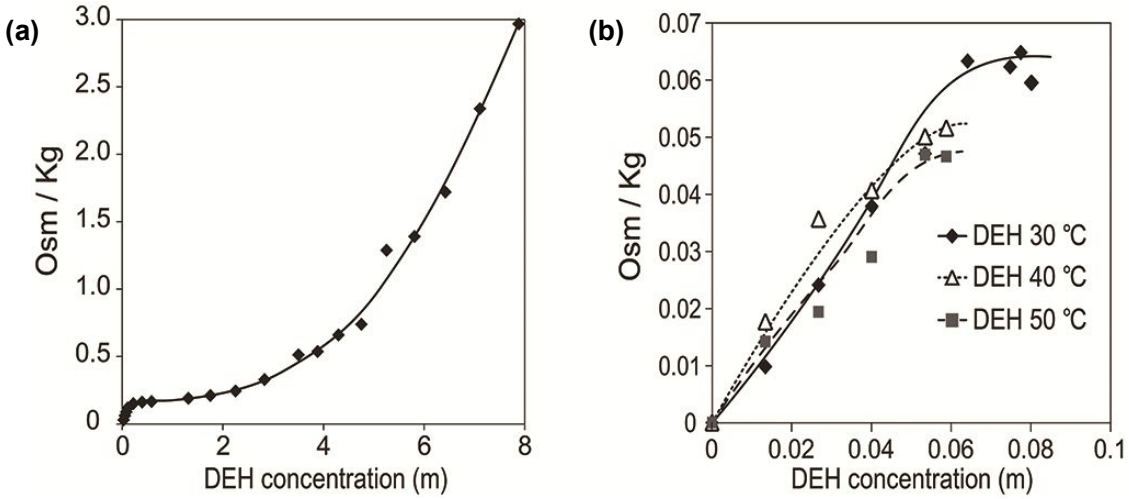

Fig. 6 Osmolality of DEH/water mixture at various concentrations (a) at low T measured by freezing point depression and (b) at high T measured by vapor pressure depression.

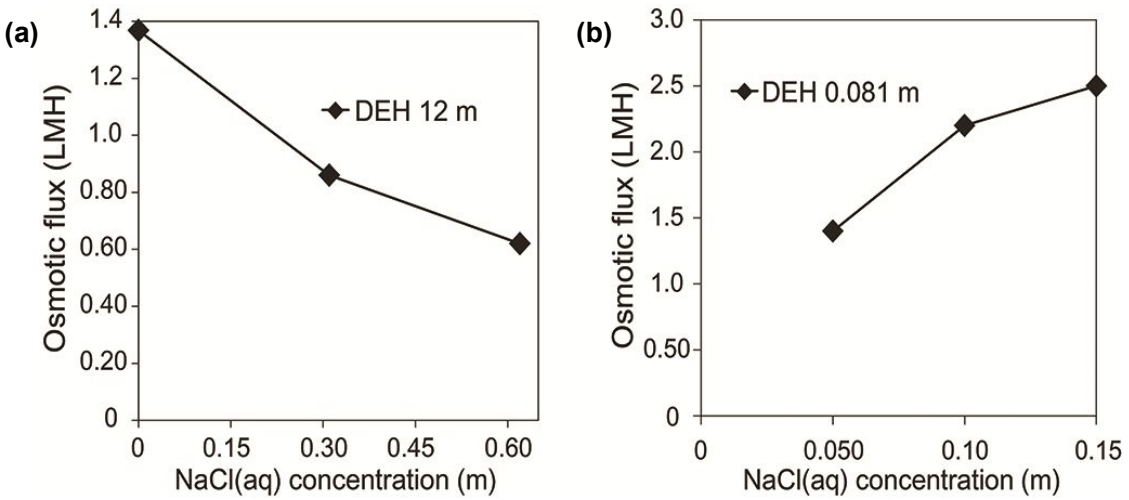

Fig. 7 Osmotic flux between the DEH aqueous solution and NaCl solutions at (a) 10 and (b) 30 °C. (a) The flow from the NaCl solution to a12 m DEH solution. (b) The flow from the 0.081 m DEH solution (*i.e.*, water-rich phase) to the NaCl solution.

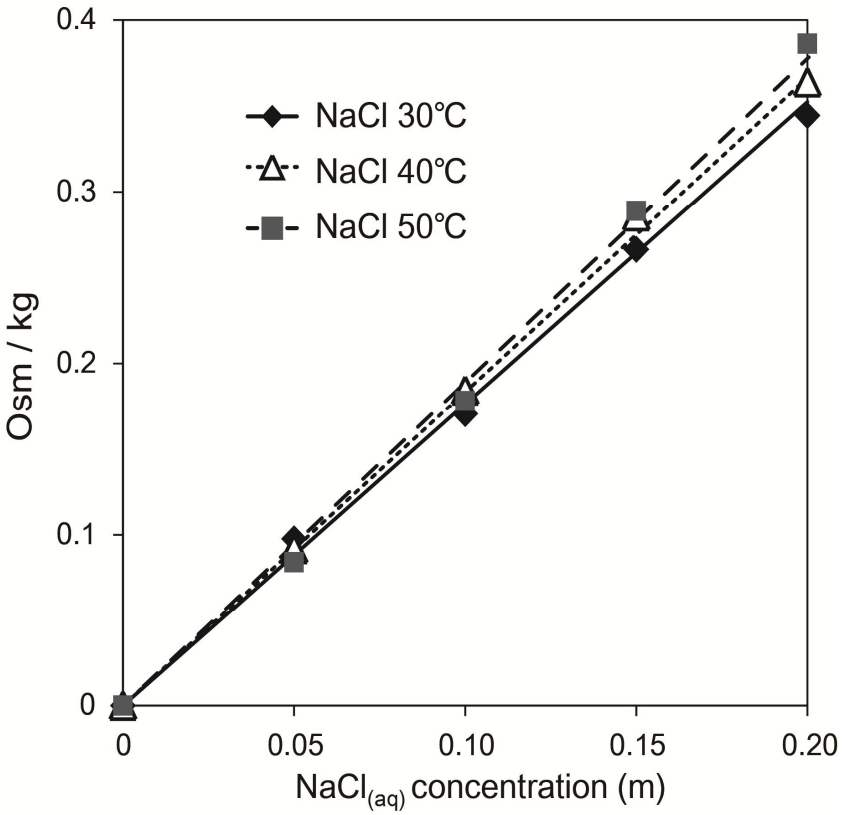

Fig. 8 Osmolality of $NaCl_{(aq)}$ solution.

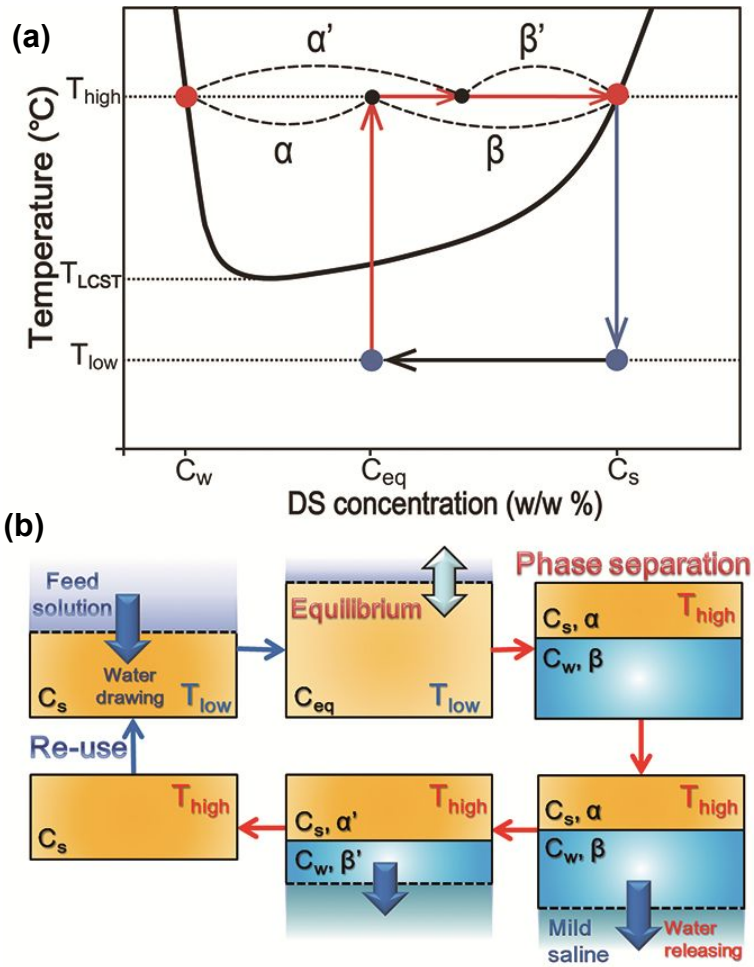

Fig. 9 Illustration of a FO desalination process by a phase diagram and a schematic diagram describing relative concentrations and amounts of each phase. DS: draw solute; T_{LCST}: LCST temperature; T_{high} and T_{low}: operation temperatures (high T and low T); C_s: the DS concentration in the draw solute-rich phase after phase separation at T_{high}; C_w: the DS concentration in the water-rich phase after phase separation at T_{high}; C_{eq}: the DS concentration of draw solution with an equivalent osmotic pressure to the feed solution.

국문 초록

저임계용해온도 (lower critical solution temperature; LCST) 형태의 상전이를 나타내는 Glycol ether (GE)/water 혼합물은 작은 온도변화에 의해서 급격한 삼투압 변화가 유도되게 된다. 온도조절에 따른 삼투압변화를 이용해서 정삼투 (forward osmotic; FO) 담수화법 실험을 실시했다. 3개의 GE중에서 di(ethylene glycol) *n*-hexyl ether (DEH)가 FO 유도용질로 선정되었다. DEH/water 혼합물은 10°C에서 반투막을 통해서 바닷물과 같은 고농도의 염수로부터 삼투현상에 의해 물을 뽑아낼 수 있었다. 그리고 물을 유도한 DEH/water 혼합물은 30°C 수준에서 water-rich층과 DEH-rich층으로 나뉜다. 삼투압이 굉장히 낮아진 water-rich층은 낮은 염수로 물을 내어 놓게 되고 DEH-rich층은 처음 DEH/water 혼합물로서 복구되게 된다. 상전이 거동, water-rich층에 남은 GE 농도, DEH/water 혼합물의 삼투압, 그리고 DEH/water 혼합물과 염수 사이의 삼투 유속을 FO 담수화 실험의 구현을 위해서 분석하였다. 10°C와 30°C 사이의 작은 온도변화에 의해서 일어나는 GE/water 혼합물의 liquid-liquid 상전이는 FO 담수화의 이상적인 유도용질의 개발에 있어 굉장히 매력적인 특성이 될 것으로 기대된다.

주요어: 온도응답성 물질, 저임계용해온도 (lower critical solution temperature; LCST), glycol ether, 상평형도, 담수화, forward osmosis (정삼투법)

학번: 2011-24025